POLITECNICO DI TORINO

ISTITUTO NAZIONALE DI RICERCA METROLOGICA

Dottorato di ricerca in Metrologia XXV ciclo

Doctoral Thesis

COHERENT ANTI-STOKES RAMAN SCATTERING, SECOND HARMONIC GENERATION AND TWO-PHOTON EXCITATION FLUORESCENCE MULTIMODAL MICROSCOPE: REALIZATION, METROLOGICAL CHARACTERIZATION AND APPLICATIONS IN REGENERATIVE MEDICINE

LEONARDO MICHAEL MORTATI

Supervisor: Dr. Maria Paola Sassi

Istituto Nazionale di Ricerca Metrologica INRIM, Italy

Academic Years 2010-2012

Coherent Anti-Stokes Raman Scattering, Second Harmonic Generation and Two-Photon Excitation Fluorescence Multimodal Microscope: Realization, Metrological Characterization and Applications in Regenerative Medicine.

Leonardo Michael Mortati

PhD thesis
Politecnico di Torino and Istituto Nazionale di Ricerca Metrologica
Printed in Torino, Italy, February 2013

This thesis is dedicated to my family and to all the people who spend their lives for humanity's progress.

Abstract

In the frame of the research in biology and in particular in regenerative medicine, it is widely requested the ability to perform measurements that have a low impact on the observed biological systems. Many measurements imply sample modifications and also sample fixation avoiding living samples measurements.

In this doctoral thesis it is presented the realization of an advanced optical multimodal microscope that integrates coherent anti-Stokes Raman scattering, second harmonic generation and two-photon excitation fluorescence techniques in a single powerful tool. The combination of all these microscopy techniques in a single microscope allows gathering more information during samples imaging, implementing fluorescence technique with label free techniques.

A description of the experimental setup of the realized multimodal microscope is presented together with the metrological characterization of the instrument, evaluating the main uncertainty sources that influence the measurement processes.

Label free microscopy techniques allow performing measurements on biological samples with low invasiveness, since to image the specimens it is not demanded any specific sample preparation. This characteristic leads to measurements on living samples with a true low impact, opening new avenues on the research in biology and in particular way in regenerative medicine.

Novel applications of these microscopy techniques are presented to study the extracellular matrix production in both fixed and living samples, as well as to characterize the scaffolds topology and the scaffold-cells interactions in a time-lapse experiment using living samples.

This doctorate thesis is composed by a state of the art chapter in which are discussed the advanced nonlinear optical microscopy techniques from a theoretical point of view, the main experimental implementations of CARS microscopy and the main parameters and properties to be measured relevant in regenerative medicine applications and products.

A chapter is dedicated to the experimental setup for the realization of the multimodal CARS-SHG-TPEF microscope at the I.N.Ri.M. laboratory.

A specific chapter is dedicated to the study of the main sources of uncertainty of the measurements using CARS, TPEF and SHG techniques.

A chapter in which are discussed the biological experiments realized using the multimodal CARS-SHG-TPEF microscope and at the end a final chapter with the conclusion of this doctorate thesis.

This study has been conducted at the Italian institute of metrology (Istituto Nazionale di Ricerca Metrologica, I.N.Ri.M.) as part of the projects REGENMED, METREGEN and ACTIVE with funding respectively from the UE (ERA-NET plus Grant Agreement No 217257) and from Piedmont Region on UE under the programs CIPE 2007- converging technologies, grant 0126000010-METREGEN and POR-FESR I-I.1.3-I1.1 - ACTIVE.

The main accomplished results are:

- The development of the whole experimental multimodal CARS-SHG-TPEF microscopy system
- The theoretical study of the main sources of uncertainty in the measurements with CARS, TPEF and SHG techniques.
- The realization of biological experiments using these microscopy techniques:
    - To study the collagen production from fixed histological sections of human dermal fibroblasts cultured in fibrin gel scaffold using CARS and SHG techniques
    - To study the collagen production by live human fibroblasts and mesenchymal stem cells cultured in fibrin gel scaffold using CARS and SHG techniques
    - To characterize polymeric scaffolds in culture media with a label-free method using CARS and SHG techniques
    - To study the colonization in a two days time-lapse experiment of a polymeric scaffold by human mesenchymal stem cells stained with calcein using CARS and TPEF techniques

Contents

List of Figures

List of Tables

1. Introduction

Optical imaging microscopy techniques are widely used as tools and methodologies in many researches and analyses in the fields of biology, pharmaceuticals, material sciences, forensic science, nanotechnologies, etc.

Generally, optical microscopy methodologies are employed to characterize biological samples and to measure for example their physical parameters (sizes, surfaces, morphology, etc.), their biological properties (cell viability, proliferation, signalling, etc.), their chemical properties (molecular biology, proteins, lipids, nucleic acids) or their mechanical parameters (structures, topology, porosity, etc.).

Since the discovery of the cells till nowadays, imaging techniques allowed tremendous progresses in biology. The technologies advanced from the traditional techniques based on transmitted light microscopy and today, fluorescence microscopy based on fluorescent probes that identify the specific biomarkers, is widely used.

However until now there is a lack of studies that evaluate and guarantee the reproducibility and the accuracy of biological measurements specifically addressed to these techniques, together with a general lack of traceability to the International System of units SI. This implies that all the measurements in medical and industrial frames that actually need a strong accuracy, are repeated a large number of times to overcome, with a statistical approach, the lack of a strong metrology. Examples of these solutions are the high-throughput screening (HTS) techniques that allow performing more than 100000 tests per day with last technology progresses. Although these techniques allow understanding the interaction or the meaning of particular biochemical processes in biological systems, this approach leads to very high costs in industrial production chains and in products quality tests. Moreover, biomedical research and in particular, regenerative medicine research, need the development of new techniques that reduce the invasiveness of the measurement methods. A specific activity on this field has been demanded to the National Metrology Institutes (NMI) to give a metrological support to the measurement in the biosciences [1].

Metrology in the bioscience will place the basis of accurate and confident quality control and quality assurance of new products from biotechnology [2]. This will lead to improve strongly the knowledge related to biological processes and to guarantee a better comparison between laboratories reducing the risks of data manipulations and the risks for the public health.

In this doctorate thesis it is proposed the development of advanced nonlinear optics microscopy techniques with low invasiveness, namely: coherent anti-Stokes Raman scattering (CARS), second harmonic generation (SHG) and two-photon excitation fluorescence (TPEF). Moreover, the metrological analysis referred to the microscopy measurements is presented together with some specific innovative applications that make use of these microscopy techniques to measure some parameters of great importance in the regenerative medicine.

This study has been conducted at the Italian institute of metrology (Istituto Nazionale di Ricerca Metrologica, I.N.Ri.M.) as part of the projects REGENMED, METREGEN and ACTIVE with funding respectively from the UE (ERA-NET plus Grant Agreement No 217257) and from Piedmont Region on UE

under the programs CIPE 2007- converging technologies, grant 0126000010-METREGEN and POR-FESR I-I.1.3-I1.1 - ACTIVE.

The main accomplished results are:

- The development of the whole experimental multimodal CARS-SHG-TPEF microscopy system
- The theoretical study of the main sources of uncertainty in the measurements with CARS, TPEF and SHG techniques.
- The realization of biological experiments using these microscopy techniques
    - To study the collagen production from fixed histological sections of human dermal fibroblasts cultured in fibrin gel scaffold using CARS and SHG techniques
    - To study the collagen production by living human fibroblasts and mesenchymal stem cells cultured in fibrin gel scaffold using CARS and SHG techniques
    - To characterize polymeric scaffolds in culture media with a label-free method using CARS and SHG techniques
    - To study the colonization in a two days time-lapse experiment of a polymeric scaffold by human mesenchymal stem cells stained with calcein using CARS and TPEF techniques

During the realization of these results also these derived products have been developed:

- Software to control the optical spectrum analyser in order to gather data for the spectral characterization in the infrared region of the filter used based on Labview.
- Software to control the excitation sources wavelength and perform automatic measurements of CARS spectra and TPEF intensity spectra versus excitation wavelength based on Labview.
- An electronic circuit that realizes the transimpedance amplifier of the photomultiplier tube (PMT) output current.
- A filter holder that reduces stray light towards the PMT in forward detection.
- An objective holder with all the necessary degrees of freedom for precise optical alignment during microscopy forward detection.
- A complete shield in aluminium that prevents stray light from the environment during the microscopy measurements.
- Algorithms to perform automatic image analyses.
- An incubator to be placed on the microscopy stage in order to allow multi-day time-lapse experiments.

Some of the accomplished results have also characteristic of originality namely:

- For the first time in Italy have been conducted biological sample imaging using CARS microscopy and combination of CARS technique with SHG or TPEF techniques.
- The proposed method for collagen produced by living stem cells in culture detection using SHG technique as a first signal of cellular differentiation in a non-invasive and non-destructive way.
- The proposed method to use CARS microscopy to characterize scaffolds in culture medium analysing also the cells migration and colonization in a time-lapse experiment using TPEF microscopy.
- The theoretical study of the main sources of uncertainty in the measurements with CARS, TPEF and SHG techniques.

This doctorate thesis is composed by a state of the art chapter in which are discussed the advanced nonlinear optical microscopy techniques from a theoretical point of view, the main experimental implementations of CARS microscopy and the main parameters and properties to be measured relevant in regenerative medicine applications and products.

A chapter is dedicated to the experimental setup for the realization of the multimodal CARS-SHG-TPEF microscope at the I.N.Ri.M. laboratory.

A specific chapter is dedicated to the study of the main sources of uncertainty of the measurements using CARS, TPEF and SHG techniques.

A chapter in which are discussed the biological experiments realized using the multimodal CARS-SHG-TPEF microscope and at the end a final chapter with the conclusion of this doctorate thesis.

2. State of the Art

Advanced nonlinear optical microscopy techniques

The progress in laser technologies with the realization and the spread of ultrafast pulsed lasers has also pushed the realization and the development of new optical microscopy techniques based on non-linear optics (NLO) phenomena.

The combination of pulsed lasers with laser scanning microscopy has opened a wide variety of NLO techniques such as for example coherent anti-Stokes Raman scattering (CARS), two-photon excitation fluorescence (TPEF) and second harmonic generation (SHG).

The excitation source optimal for CARS microscopy allows also exciting other non-linear optical processes that could be exploited and implemented in the same microscope in order to get more information from the sample. In this way, with a single tool is possible to use more microscopy techniques simultaneously and for this reason this collection of techniques is called multimodal microscopy.

CARS microscopy allows label-free and chemically selective imaging of the sample in a non-invasive way since no special samples preparations are needed.

Two-photon excitation fluorescence can be used to observe fluorescent tags inside the specimens that can be expressed by the sample itself (fluorescent proteins or endogenous autofluorescence in cells) or added during the sample preparation.

Second harmonic generation is a process that allows observing materials with a non-centrosymmetric molecular structure, since these materials under specific conditions can double the frequency of an impinging light radiation. SHG can be also considered a label-free non-invasive and chemically selective technique and samples can be imaged without any special preparations.

Coherent Anti-Stokes Raman Scattering Microscopy

When a monochromatic radiation impinges a molecular system the light can experience three possible effects: absorption, transmission and scattering. When a molecule absorbs light, the kinetic energy of the hitting photon is completely transferred to the molecular system; when the light is transmitted through the material, the hitting photon passes the material lattice without any perturbation.

The scattering is a process that involves absorption and re-emission of a photon by the molecular system. The scattering could be elastic if the same amount of absorbed kinetic energy is re-emitted (Rayleigh scattering), or inelastic if the kinetic energy of the re-emitted photon is different from that of the hitting photon. Raman scattering is an example of inelastic scattering. If the material absorbs part of the impinging photon energy, the new re-emitted photon will be red shifted with respect to the hitting one and the energy difference is converted in vibrations or rotations of molecule (Stokes Raman scattering shift). If the re-emitted photon absorbs some kinetic energy from the vibrations or rotations of the molecule, it will be blue-shifted with respect to the hitting photon (anti-Stokes Raman scattering shift).

The scattering is an induced secondary emission process and photons can be re-emitted in any directions independently by the direction of the hitting photon that originated the process. The Raman scattering process admits that the molecular system can be excited at an energy level very unstable called "virtual level" that has a very short lifetime of about 10^{-14} second, just enough to allow the photon absorption and re-emission. This phenomena makes Raman scattering different from the fluorescence process since in fluorescence the absorption of a photon, drives the molecule in an excited state that then relaxes vibrationally and electronically in lower energy states with a decay time several order larger than that of Raman scattering.

The Raman spectroscopy is a technique that exploits the Raman scattering processes to investigate the vibrational or rotational modes of molecules, looking at the frequency shifts of the scattered photons. However, in normal conditions, only a very small part of photons impinging a molecular system are scattered inelastically (about one out of a million) and thus the efficiency of this process is very low.

Raman process is related to the polarizability α of a molecule electron cloud and a Raman transition can be activated only in presence of non-zero polarizability with respect to the normal coordinates generally expressed as *Q,* representing molecule vibrations or rotations.

In the classical framework for the understanding of the Raman scattering process, a photon may be thought also as an electromagnetic radiation that interacting with a material induces a dipole moment *P*:

$$P = \alpha \bar{E} \tag{1}$$

Where α is the polarizability of the material and $\bar{E}$ is the strength of the electric field of the incident photon. For the incident photon, the electric field may be expressed as:

$$\bar{E} = E_0 \cos(2\pi\omega_0 t) \tag{2}$$

Where ω_0 is the frequency of the incident photon ($\omega_0 = \frac{c}{\lambda}$). If (2) is substituted into (1) yields the time-dependent induced dipole moment:

$$P = \alpha E_0 \cos(2\pi\omega_0 t) \tag{3}$$

The polarizability is a function of the instantaneous position of the constituent atoms of the molecular structure and for every molecular bond the atoms are confined under specific vibrational modes. The vibrational modes have quantized energy and thus only particular vibrational frequencies ω_{vib}. The physical displacement dQ of the atoms due to the particular vibrational modes may be expressed as:

$$dQ = Q_0 \cos(2\pi\omega_{vib} t) \tag{4}$$

Where Q_0 is the maximum displacement about the equilibrium position that typically doesn't exceed the 10% of the overall bond length. In the condition of small displacements, the polarizability may be approximated by a Taylor series expansion truncated at the first term,

$$\alpha = \alpha_0 + \frac{\partial \alpha}{\partial Q} dQ \tag{5}$$

Substituting the eq. (4) into (5) the polarizability is given by:

$$\alpha = \alpha_0 + \frac{\partial \alpha}{\partial Q} Q_0 \cos(2\pi\omega_{vib} t) \tag{6}$$

Using the above relation (6) the induced dipole moment (3) may be written as:

$$P = \alpha E_0 \cos(2\pi\omega_0 t) + \frac{\partial\alpha}{\partial Q} Q_0 E_0 \cos(2\pi\omega_0 t)\cos(2\pi\omega_{vib} t) \quad (7)$$

After recasting using a trigonometric identity the eq. (7) may be written as:

$$P = \alpha E_0 \cos(2\pi\omega_0 t) + \left(\frac{\partial\alpha}{\partial Q}\frac{Q_0 E_0}{2}\right)\{\cos[2\pi(\omega_0 - \omega_{vib})t] + \cos[2\pi(\omega_0 + \omega_{vib})t]\} \quad (8)$$

The last relation shows that the induced dipole moment has three different frequency components, that are ω_0, $(\omega_0 - \omega_{vib})$, and $(\omega_0 + \omega_{vib})$, which determine the possible frequencies of the scattered radiation. The first scattered frequency ω_0 coincides with the frequency of the incident radiation and it is related to the Rayleigh elastic scattering. The latter two frequencies $(\omega_0 - \omega_{vib})$, and $(\omega_0 + \omega_{vib})$ differ from the frequency of the incident radiation and are related to the inelastic Raman scattering. It must be taken into account that inelastic Raman scattering may exist only if the term $\frac{\partial\alpha}{\partial Q}$ differs from zero. This means that a vibrational mode can be Raman active only if there is a change in the polarizability during the vibrational displacement of atoms. This characteristic makes Raman scattering generally more suitable to detect symmetric vibrations of non-polar groups.

Coherent anti-Stokes Raman scattering process

Coherent anti-Stokes Raman Scattering (CARS) is a four waves mixing process that differs from the spontaneous Raman scattering process because the vibrational modes of the material are coherently driven by beating of two optical waves instead of thermal excitation. The CARS signal is directly related to the third order non-linear susceptibility $\chi^{(3)}$, which exhibits resonances of the material. Although CARS is a process that involves three excitation waves, in most of the practical implementations two of the three waves have the same frequency, so that two optical beams do actually interact (provided that one of them, the so called pump wave, contributes to the interaction with two photons).

The energy diagram of a typical CARS process with the involved level transitions is shown in Fig. 2.1 (right side), together with that of spontaneous Raman scattering in its Stokes and anti-Stokes forms (left side). The Raman active vibrational transition occurs at frequency ω_R. The pump wave has frequency ω_p, whereas the second excitation wave, the Stokes wave is placed at $\omega_S = \omega_p - \omega_R$; the CARS wave occurs at $\omega_{aS} = \omega_p + \omega_R = 2\omega_p - \omega_S$.

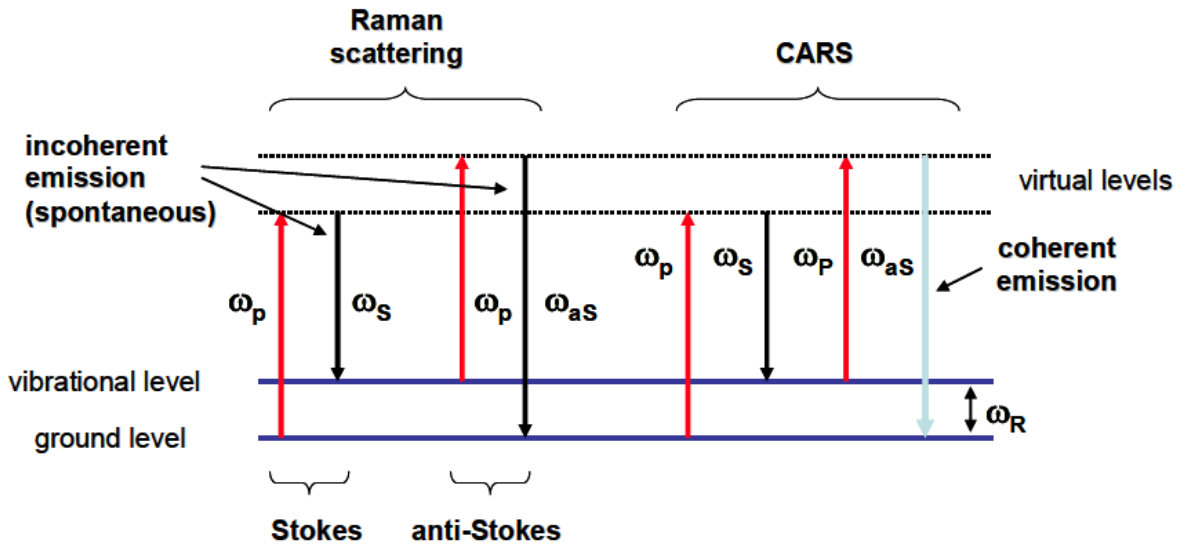

Fig. 2.1 Energy diagrams of spontaneous Raman scattering (left) and CARS (right).

In CARS the Raman active mode of the material is coherently driven (hence the name of the effect) by the beating of the pump and Stokes wave at $\omega_R = \omega_p - \omega_S$. The CARS wave at ω_{aS} results from the inelastic scattering of the wave at ω_p by the molecular vibrations coherently driven by the beating. For the sake of completeness it must be noted that a similar mechanism creates, for reasons of symmetry, another wave at $\omega_{cS} = 2\omega_S - \omega_R$ (Coherent Stokes Raman Scattering, CSRS). In the case of the CSRS the material before and at the end of the scattering process needs to be in an excited vibrational level. This condition makes the detection of this wave more difficult than that of the anti-Stokes wave.
CARS signal being coherently driven by the excitation sources is several orders stronger than spontaneous Raman, allowing faster microscopic and spectroscopic analyses than spontaneous Raman.
Finally, it should be noted that the waves at ω_p and ω_S are directly coupled by Stimulated Raman Scattering (SRS), and experience either gain or loss. These properties form the basis for Stimulated Raman Gain (or Loss) Spectroscopy [3-5].

In the simple case where the interacting fields are described as plane waves propagating along the z axis normal towards a slab of nonlinear material of thickness L, assuming negligible depletion of the excitation fields (pump and Stokes signals) and negligible loss into the material, the solution of the coupled propagation equations for the interacting fields is straightforward [6].
In particular the following expression for the anti-Stokes (CARS) signal intensity exiting the nonlinear slab, $I_{aS}(\omega_{aS}, L)$, is obtained:

$$I_{aS}(\omega_{aS}, L) = \frac{9\omega_{aS}^2}{16\varepsilon_0^2 c^4 n(\omega_{aS}) n(\omega_S) n^2(\omega_p)} \left|\chi^{(3)}(\omega_{aS})\right|^2 I^2(\omega_p, 0) I(\omega_S, 0) L^2 \frac{\sin^2\left(\frac{1}{2}\Delta k L\right)}{\left(\frac{1}{2}\Delta k L\right)^2} \quad (9)$$

Where the phase mismatch Δk and the non-linear susceptibility are given respectively by:

$$\Delta k = k_{aS} - (2k_p - k_S) \quad (10)$$

$$\chi^{(3)}(\omega_{aS}) = \vec{e}_{aS} \chi^{(3)} : \vec{e}_p \vec{e}_p \vec{e}_S \quad (11)$$

($k_i = \frac{2\pi n_i}{\lambda_i}, i = p, S, aS$; the vectors $\vec{e}_i$ are the unit vectors of the polarization direction of the various fields; the nonlinear susceptibility is in general a four-rank tensor, and the two dots indicate tensor product).
The oscillating term depending on the phase mismatch Δk takes into account the coherent nature of the generation process, where the final signal builds up from coherent addition of the waves generated at different positions along the slab of non-linear material. If the phase-matching condition is not satisfied, $\Delta k \neq 0$, part of the radiation generated along the sample will interfere destructively between each other, so that the output becomes weaker and depends critically on the sample thickness *L* as discussed below. The observed CARS intensity is maximum when phase matching with the excitation beams is achieved *(*$\Delta k = 0$); the intensity is proportional to the square of the intensity of the pump field, depends linearly on the intensity of the Stokes field.
The CARS signal intensity depends on the square modulus of the third-order non-linear susceptibility of the material, $\chi^{(3)}$. This is another important feature affecting the spectral behaviour of the CARS emission. In general, the third order susceptibility is made of non-resonant contributions lumped in the term $\chi_{NR}^{(3)}$, and resonant contributions as follows:

$$\chi^{(3)}_{1111}(\omega_{CARS} = 2\omega_p - \omega_S) = \chi^{(3)}_{NR} + \\ + \frac{A_{TP}}{\omega_{TP} - 2\omega_p - i\Gamma_{TP}} + \frac{A_{TP}}{\omega_{TP} - 2\omega_S - i\Gamma_{TP}} + \frac{A_{TP}}{\omega_{TP} - (\omega_p + \omega_S) - i\Gamma_{TP}} + \\ + \sum_R \frac{A_R}{\omega_R - (\omega_p + \omega_S) - i\Gamma_R} \tag{12}$$

Where the three terms on the second line are resonant contributions due to two-photon processes produced by the pump and Stokes beams whereas the terms on the third line are resonant contribution due the Raman transitions. The A_R terms are constants related to the mode density and the Raman cross sections of the various active transitions, whereas $2\Gamma_R$ is the corresponding linewidth.

In practice, when using pump and Stokes signal in the near IR the two-photon processes are far from resonance and can be lumped in the non-resonant term. If, finally, in the observation region there is only one active Raman resonance, at ω_R, the third order susceptibility could take the form:

$$\chi^{(3)}_{1111} = \chi^{(3)}_{NR} + \chi^{(3)}_R = \chi^{(3)}_{NR} + \frac{A_R}{\omega_R - (\omega_p - \omega_S) - i\Gamma_R} = \chi^{(3)}_{NR} + \frac{A_R}{\Delta - i\Gamma_R} = \chi^{(3)}_{NR} + \frac{A_R \Delta}{\Delta^2 - i\Gamma_R^2} - i\frac{A_R \Gamma_R}{\Delta^2 - \Gamma_R^2} \tag{13}$$

Where $\Delta = \omega_R - \omega_p + \omega_S$ is the *detuning* from the Raman resonance frequency. The third order susceptibility being a complex number, several terms come in to play in the expression for the CARS intensity, namely:

$$\left|\chi^{(3)}_{1111}\right|^2 = \left|\chi^{(3)}_{NR}\right|^2 + \frac{A_R^2}{\Delta^2 + \Gamma_R^2} + \frac{2A_R \chi^{(3)}_{NR} \Delta}{\Delta^2 + \Gamma_R^2} \tag{14}$$

From eq. (14) appears clearly that the shape of the CARS spectrum is different from that of the Raman spectrum of the vibrational transition obtained traditionally. The CARS spectrum has a marked dispersive character and the emission peak is shifted with respect to the Raman emission line ($\Delta = 0$) , depending on the linewidth of the Raman transition.

The CARS spectrum is therefore asymmetrical with respect to the active Raman resonance ω_R. The point where the CARS spectrum crosses the value of the non resonant background does not correspond to the actual Raman resonance. Examples of calculated CARS spectra are given in Fig. 2.2 for various values of the Raman linewidth Γ_R (0.5, 1 e 2 cm^{-1}). In the figures on the left, the real part (red curve) and the imaginary part (blue curve) of the third order susceptibility are depicted together with $\left|\chi^{(3)}_{NR}\right|^2$ (green curve). The Raman spectrum is proportional to the square of the imaginary part of $\chi^{(3)}$ (blue curves). The resulting CARS spectra are given in the figures on the right.

It is important to note that for positive detuning there is a region where there is destructive interference between the CARS signal and the background radiation giving an intensity of the resulting signal lower than that of the background.
The square dependence of CARS intensity on the third order non-linear susceptibility also implies that the generated intensity is proportional to the square of the density of the chemical species under study. This aspect is to be kept in mind when using CARS spectroscopy for quantitative analysis of specimens.

The CARS signal can be detected in forward (k_{AS} along z), forward CARS (F-CARS), and backward direction (k_{AS} along –z), E-CARS. The phase matching condition, $\Delta kL \ll \pi$ can be fulfilled if $\Delta k \approx 0$ or $L \approx 0$. It is important to note that for a very thin sample ($L \sim 0$), the phase matching condition is realized in both the